Test Report of Heavy-ion SEEs for the LTC6400-20 Differential ADC Driver

Test Date: May 23th – 26th, 2009

Principal Investigator: Dakai Chen, MEI Technologies/GSFC
Test Engineer: Hak Kim, MEI Technologies/GSFC

I. Introduction

The purpose of this study is to examine the heavy-ion-induced single-event-effects (SEEs) susceptibility of the LTC6400-20 differential amplifier manufactured by Linear Technology.

II. Device Description

The LTC6400-20 is a high-speed differential amplifier, based on SiGe technology, designed to drive 12-, 14-, and 16-bit ADCs. The device features a fixed gain of 10 V/V (20 dB), and a -3dB bandwidth up to 1.8 GHz. The test/part information is listed in Table 1. The device specifications are listed in Table 2.

Table 1. Test and part information

Generic Part Number	LTC6400-20
Full Part Number	746 LCCS N112 705 LCCS N016
Manufacturer	Linear Technology
Lot Date Code (LDC)	746 and 705
Quantity tested	2
Part Function	Differential amplifier
Part Technology	Silicon-Germanium
Package Style	16-lead QFN
Test Equipment	Power supply, RF generator, high-speed oscilloscope
Test Engineer	Hak Kim

Table 2. Device specifications

Parameter	Test Conditions	Min	Typ	Max	Unit
Gain*	V_{IN} = ±100 mV Differential	19.4	20	20.6	dB
Supply Voltage (V_S)		2.85	3	3.5	V
Supply Current (I_S)	$\overline{\text{ENABLE}}$ = 0.8V	75	90	105	mA
Shutdown Supply Current (I_{SHDN})	$\overline{\text{ENABLE}}$ = 2.4V		1	3	mA

* The actual gain measured at the output of the demo board will be ~14 dB.

III. Test Facility

Facility: Texas A&M University Cyclotron SEE Test Facility

Beam Energy: 15 MeV/amu
Flux: 5×10^4 to 1×10^5 particles/cm^2/s
Fluence: $\leq 2 \times 10^7$ particles/cm^2
Ions:

Table 3. Heavy ion specifications.

Ion	Peak Energy (MeV)	LET (MeV·cm^2/mg)	Range in Si (µm)
Ar	29	7.4	229
Kr	152	24.8	170

IV. Test Method

Figure 1 shows the test circuit designed for single-ended input operation. The application circuit uses input and output transformers for single-ended-to-differential conversion and impedance transformation. The -3dB bandwidth is reduced from 1.8 GHz to 1.3 GHz as a result of the transformers. A block diagram of the test setup is shown in Figure 2. A computer is programmed to observe and capture the SETs.

The irradiation was performed for each ion species at 0^o (normal incidence), 45^o and 60^o angles. The layer specifications used for the SEUS (Single Event Upset System Supervisor) software were approximated: SiGe, SiO_2 (1µm), air gas (70 mm), and aramica (1 mil). A high-speed digital oscilloscope was connected to the output of the board to capture any single-event-transient (SET). Each part was irradiated until 100 transients were observed or up to a fluence of 2×10^7 ions/cm^2. Figure 3 shows photographs of the delidded part and the demo board.

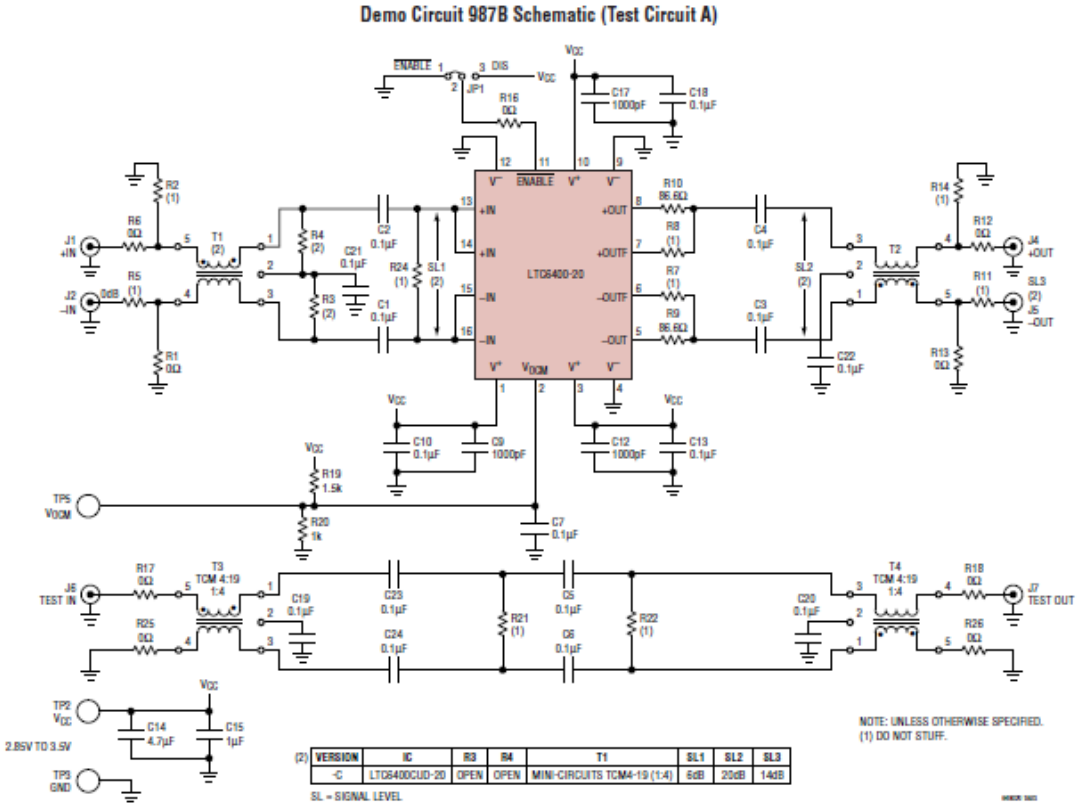

Figure 1. Application circuit configuration.

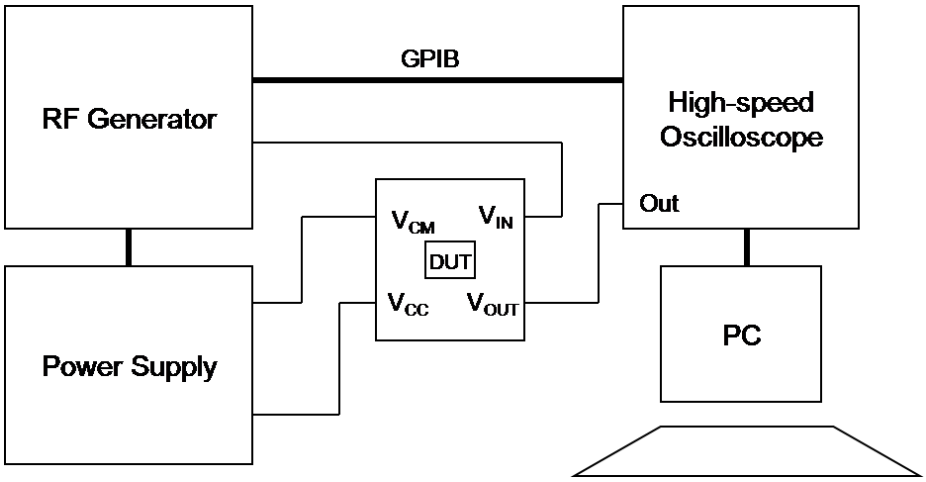

Figure 2. Test setup block diagram.

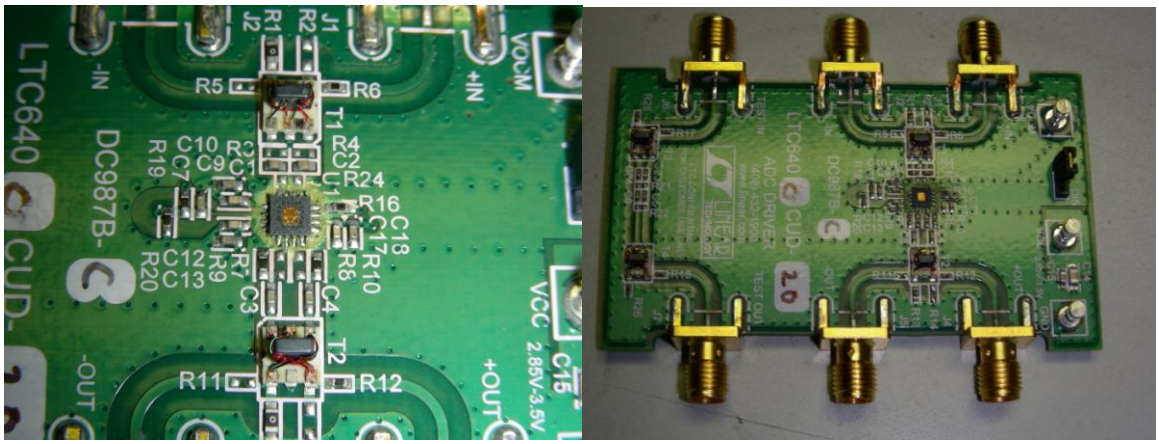

Figure 3. Photograph of a delidded part and the test board.

Test Conditions

Test temperature:	Ambient temperature
Operating frequency:	10, 100, and 1000 MHz
Supply voltage:	V_{CC} = 3 V, V_{CM} = 1.25 V
Input Voltage:	140 mV_{pp}, sine wave, and 2 mV_{pp} sine wave for small signal response
Parameter:	(1) The SET trigger on large signals was set to ±10% of 1/2 of the pulse period. The SET trigger on small signals was set to +10 mV. SET tests were run until 100 transients are observed and acquired, or up to a fluence of 2×10^7 ions/cm^2. (2) Supply currents. (3) Single-Event-Latchups were also monitored.
Data format:	Spreadsheet
Beam hours:	**8**

V. Results

Figure 4 shows the SET cross-sections from large signal responses at 10, 100, and 1000 MHz. The ion species and angles of irradiation are also indicated in the figure. The SET cross-section increases by ~1 order of magnitude for each increase of one magnitude in frequency. The SET LET threshold is less than 7.4 MeV·cm^2/mg. We observed very few transients (1-2) for the 10 MHz large signal at the lowest LET of 7.4 MeV·cm^2/mg, up to a fluence of 2×10^7 ions/cm^2. The curves do not appear to saturate up to an LET of 49.6 MeV·cm^2/mg. However the upset cross-section increases only gradually with LET.

Figures 5 – 10 show various SETs for large signals of different frequencies at LETs of 7.4 and 49.6 MeV·cm^2/mg. The transient characteristics are similar for different LET values. However the transient shapes depend significantly on frequency. SETs at 10 MHz appeared as small glitches, as shown in Figures 5 and 6. The majority of SETs at 100 MHz are positive- or negative-going voltage spikes, as shown in Figure 7 and 8. A few SETs at 100 MHz disrupts several cycles of the signal, as shown in Figure 9. Most SETs occurring at 1000 MHz completely "erase" the signal for several cycles, as shown in Figure 10. The types of SETs exhibited in Figures 9 and 10 could have severe impact on device performance, as several bits of data are affected.

The small signal radiation performance was also evaluated. A 2 mV_{pp} sine wave was used as the input. Figures 11 and 12 show the worst case SETs from 10 and 1000 MHz. Unlike the large signal response, the transient characteristics are similar for the different frequencies. The SET upset rates are also similar for different frequencies for the small signals. Figure 13 shows the SET cross-sections from the small signal response at 10 and 1000 MHz.

No latchup events were observed. The supply current values remained relatively unchanged, at ~92−94 mA, throughout irradiation.

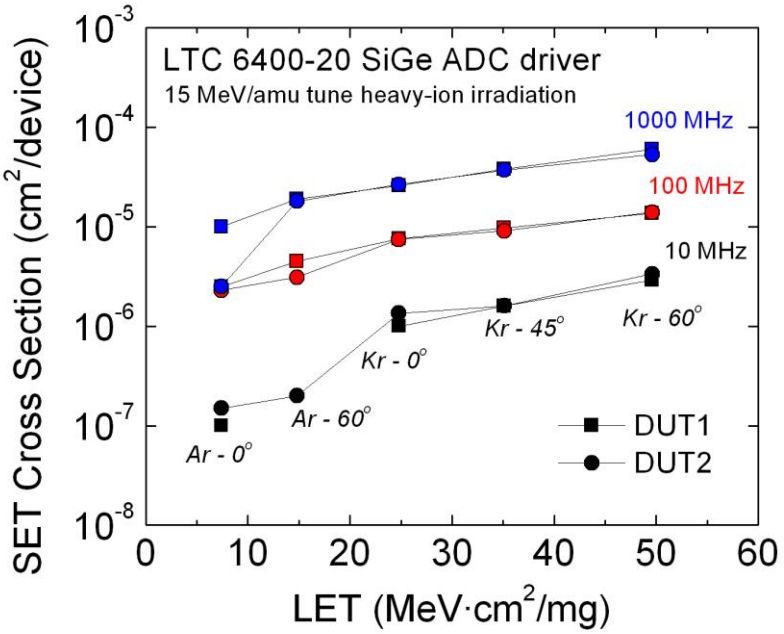

Figure 4. SET cross-sections for large signals with frequencies of 10, 100 and 1000 MHz.

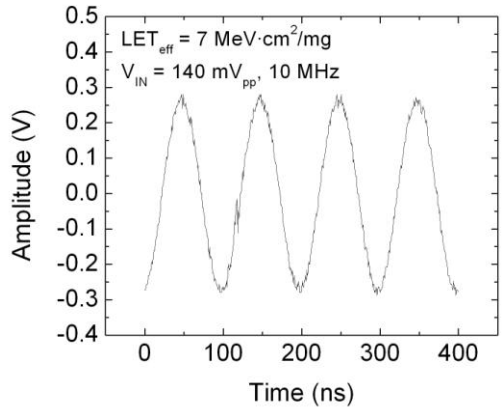

Figure 5. SET with LET_{eff} = 7.4 MeV·cm^2/mg for a 10 MHz large signal.

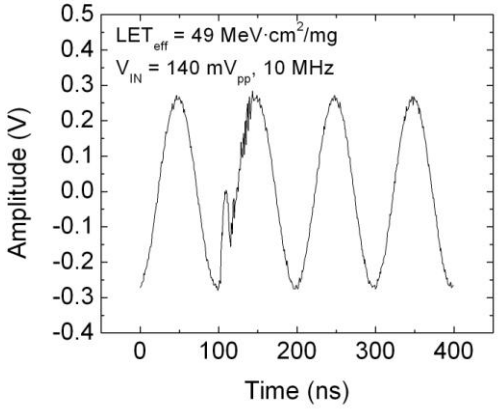

Figure 6. SET with LET_{eff} = 49.6 MeV·cm^2/mg for a 10 MHz large signal.

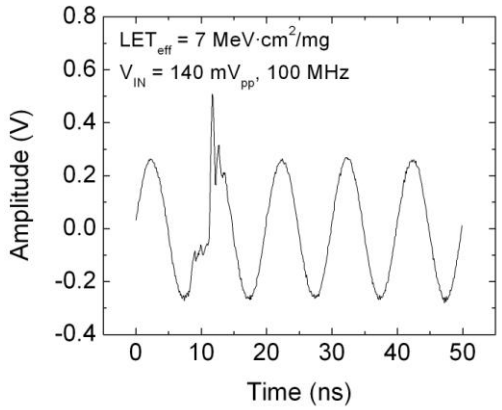

Figure 7. SET with LET_{eff} = 7.4 MeV·cm^2/mg for a 100 MHz large signal.

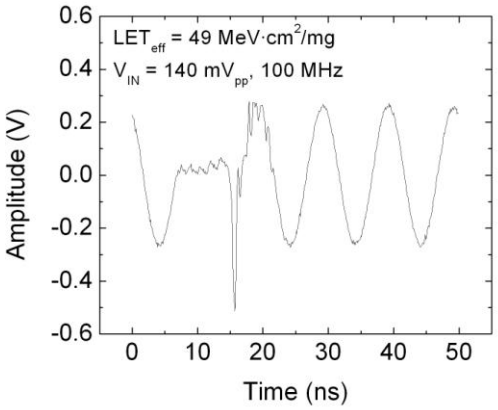

Figure 8. SET with LET_{eff} = 49.6 MeV·cm^2/mg for a 100 MHz large signal.

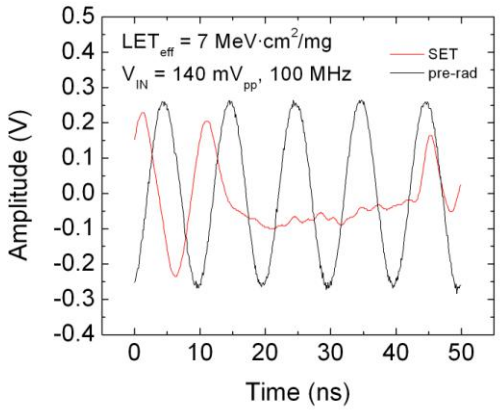

Figure 9. SET with LET_{eff} = 7.4 MeV·cm^2/mg for a 100 MHz large signal.

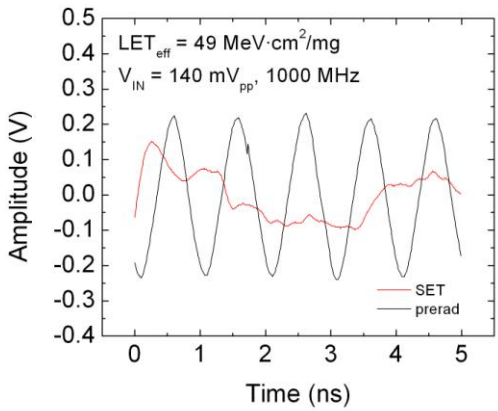

Figure 10. SET with LET_{eff} = 49.6 MeV·cm^2/mg for a 1000 MHz large signal.

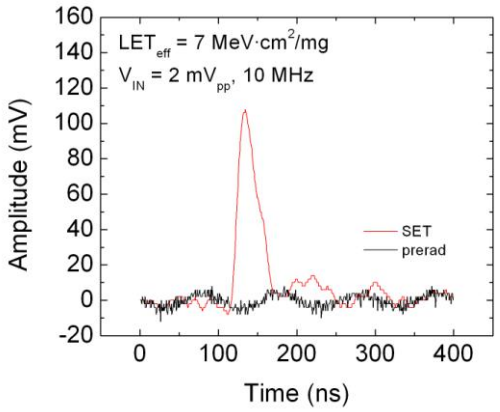

Figure 11. SET with LET_{eff} = 7.4 MeV·cm^2/mg for a 10 MHz small signal.

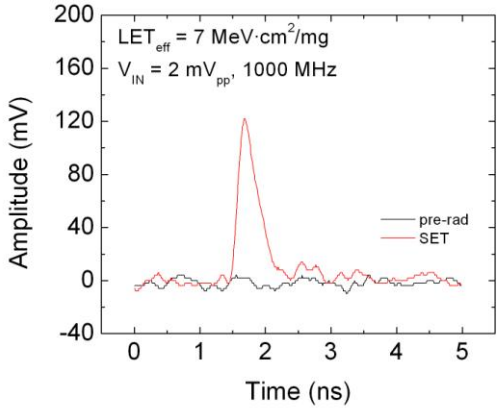

Figure 12. SET with LET_{eff} = 7.4 MeV·cm^2/mg for a 1000 MHz small signal.

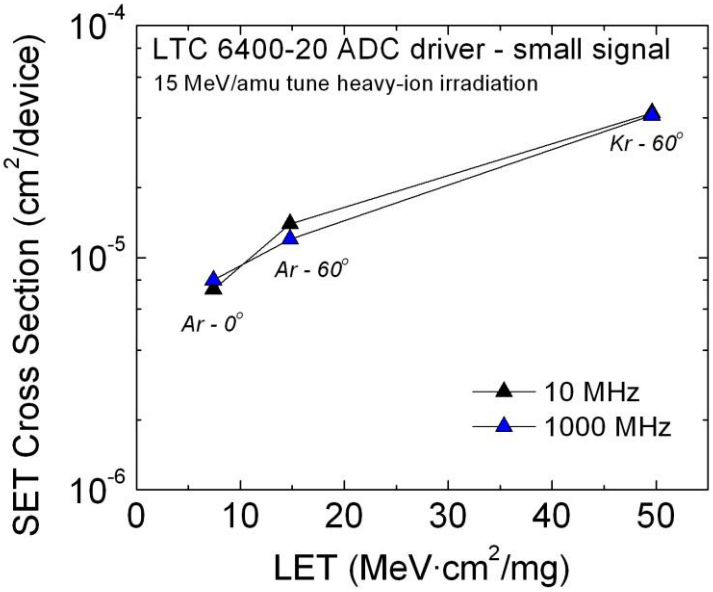

Figure 13. SET cross-sections for small signals with frequencies of 10 and 1000 MHz.

VI. Conclusions

The results showed that the LTC6400 differential output amplifier is susceptible to heavy-ion-induced SETs, with a threshold LET less than 7.4 MeV·cm^2/mg. The SET cross-sections depend on the operation frequency; the cross-section increases logarithmically with frequency. The SET characteristics also depend on frequency. SETs from 10 MHz signals are relatively minor. At 100 MHz, the SETs appear mostly as short duration voltage spikes. However at 1000 MHz, the majority of SETs "erases" the signal for several cycles. Therefore the device operation at higher frequencies will be significantly disrupted. The SETs from small signal response did not exhibit frequency dependence. The transients appeared mostly as voltage spikes.

Without implementing additional radiation hardness assurance designs, the LTC6400 may be used for space applications at relatively lower frequencies (< 100 MHz), depending on application.

VII. Appendix

LTC6400-20, Vcc=3V, Vcm=1.25V, 15 MeV Tune

Run	DUT	Frequency (MHz)	Vin (mV)	Ion	Beam Energy (MeV/amu)	LET (MeV·cm^2/mg)	Angle (deg)	Eff LET (MeV·cm^2/mg)	Flux (ions/cm2/s)	Fluence (ions/cm2)	SETs	Cross-Section
1	1	10	140	Ar	12	7.4	0	7.4	5.0E+04	1.0E+07	0	0.00E+00
2	1	10	140	Ar	12	7.4	0	7.4	5.2E+04	2.0E+07	2	1.00E-07
3	1	10	2	Ar	12	7.4	0	7.4	5.3E+04	2.0E+07	146	7.30E-06
4	1	1000	2	Ar	12	7.4	0	7.4	9.8E+04	2.0E+07	160	8.00E-06
5	1	1000	140	Ar	12	7.4	0	7.4	9.6E+04	2.0E+07	200	1.00E-05
6	1	100	140	Ar	12	7.4	0	7.4	8.8E+04	2.0E+07	50	2.50E-06
7	1	100	140	Ar	12	7.4	60	14.8	8.5E+04	2.0E+07	90	4.50E-06
8	1	10	140	Ar	12	7.4	60	14.8	8.6E+04	1.0E+07	0	0.00E+00
9	1	1000	140	Ar	12	7.4	60	14.8	8.5E+04	1.0E+07	190	1.90E-05
10	1	10	2	Ar	12	7.4	60	14.8	8.3E+04	1.0E+07	136	1.36E-05
11	1	1000	2	Ar	12	7.4	60	14.8	8.4E+04	1.0E+07	119	1.19E-05
12	2	10	140	Ar	12	7.4	60	14.8	7.3E+04	1.0E+07	2	2.00E-07
13	2	100	140	Ar	12	7.4	60	14.8	7.0E+04	1.0E+07	35	3.50E-06
14	2	100	140	Ar	12	7.4	60	14.8	6.6E+04	1.0E+07	26	2.60E-06
15	2	1000	140	Ar	12	7.4	60	14.8	1.2E+05	1.0E+07	182	1.82E-05
16	2	10	140	Ar	12	7.4	0	7.4	1.2E+05	1.0E+07	2	2.00E-07
17	2	10	140	Ar	12	7.4	0	7.4	1.2E+05	1.0E+07	1	1.00E-07
18	2	100	140	Ar	12	7.4	0	7.4	1.1E+05	1.0E+07	23	2.30E-06
19	2	100	140	Ar	12	7.4	0	7.4	1.2E+05	1.0E+07	27	2.70E-06
20	2	1000	140	Ar	12	7.4	0	7.4	1.1E+05	2.0E+07	221	1.11E-05
21	2	10	140	Kr	10.3	24.8	0	24.8	1.1E+05	2.0E+07	27	1.35E-06
22	2	100	140	Kr	10.3	24.8	0	24.8	1.1E+05	2.0E+07	149	7.45E-06
23	2	1000	140	Kr	10.3	24.8	0	24.8	1.1E+05	1.0E+07	266	2.66E-05
24	2	10	140	Kr	10.3	24.8	45	35.1	1.1E+05	2.0E+07	32	1.60E-06
25	2	100	140	Kr	10.3	24.8	45	35.1	1.0E+05	2.0E+07	182	9.10E-06
26	2	1000	140	Kr	10.3	24.8	45	35.1	9.7E+04	1.0E+07	370	3.70E-05
27	2	10	140	Kr	10.3	24.8	60	49.6	8.7E+04	2.0E+07	67	3.35E-06
28	2	100	140	Kr	10.3	24.8	60	49.6	8.4E+04	1.0E+07	140	1.40E-05
29	2	1000	140	Kr	10.3	24.8	60	49.6	7.6E+04	1.0E+07	533	5.33E-05
30	1	10	140	Kr	10.3	24.8	60	49.6	6.9E+04	2.0E+07	58	2.90E-06
31	1	100	140	Kr	10.3	24.8	60	49.6	6.6E+04	1.0E+07	137	1.37E-05
32	1	1000	140	Kr	10.3	24.8	60	49.6	6.3E+04	5.0E+06	301	6.02E-05
33	1	10	2	Kr	10.3	24.8	60	49.6	6.0E+04	5.0E+06	208	4.16E-05
34	1	1000	2	Kr	10.3	24.8	60	49.6	6.1E+04	5.0E+06	206	4.12E-05
35	1	10	140	Kr	10.3	24.8	45	35.1	5.2E+04	5.0E+06	7	1.40E-06
36	1	10	140	Kr	10.3	24.8	45	35.1	5.5E+04	1.5E+07	25	1.67E-06
37	1	100	140	Kr	10.3	24.8	45	35.1	5.5E+04	5.0E+06	49	9.80E-06
38	1	100	140	Kr	10.3	24.8	45	35.1	5.4E+04	5.0E+06	48	9.60E-06
39	1	1000	140	Kr	10.3	24.8	45	35.1	5.3E+04	5.0E+06	191	3.82E-05
40	1	10	140	Kr	10.3	24.8	0	24.8	4.4E+04	2.0E+07	20	1.00E-06
41	1	100	140	Kr	10.3	24.8	0	24.8	1.0E+05	2.0E+07	151	7.55E-06
42	1	1000	140	Kr	10.3	24.8	0	24.8	9.9E+04	1.0E+07	264	2.64E-05